Validation of FreeSurfer-Estimated Brain Cortical Thickness: Comparison with Histologic Measurements

**Francesco Cardinale · Giuseppa Chinnici · Manuela Bramerio · Roberto Mai ·
Ivana Sartori · Massimo Cossu · Giorgio Lo Russo · Laura Castana · Nadia Colombo ·
Chiara Caborni · Elena De Momi · Giancarlo Ferrigno**

F. Cardinale (✉) · R. Mai · I. Sartori · M. Cossu · G. Lo Russo ·
L. Castana
"Claudio Munari" Center for Epilepsy and Parkinson Surgery,
Niguarda Hospital, Piazza Ospedale Maggiore, 3, 20162 Milan, Italy
e-mail: francesco.cardinale@ospedaleniguarda.it

G. Chinnici · C. Caborni · E. De Momi · G. Ferrigno
Nearlab, Bioengineering Department, Politecnico di Milano,
Via G. Colombo, 40, 20133 Milan, Italy

M. Bramerio
Service of Pathology, Niguarda Hospital, Piazza Ospedale Maggiore,
3, 20162 Milan, Italy

N. Colombo
Department of Neuroradiology, Niguarda Hospital,
Piazza Ospedale Maggiore 3, 20162 Milan, Italy

Introduction

Manual or automatic cortical thickness measurement was proposed for studying epilepsy (Antel et al. 2003; Colliot et al. 2006; McDonald et al. 2008; Oliveira et al. 2010; Labate et al. 2011; Thesen et al. 2011; Widjaja et al. 2011), as well as a number of other neurological and psychiatric disorders.

FreeSurfer (Dale et al. 1999) is one of the most prominent packages for post-processing computer-aided neuroimages. It is "an array of image analysis tools designed to be automated, robust, accurate and relatively easy to use" (Fischl 2012). FreeSurfer's automated pipeline, given a T1-weighted 3D Magnetic Resonance (MR) series as input, outputs a model of hemispheric white and pial surfaces (Dale et al. 1999; Fischl et al. 2001), and an estimation of the cortical thickness, computed as the distance between the gray/white matter boundary and the pial surface for each pair of vertices of the two meshes (Fischl and Dale 2000). Rosas et al. (2002) validated the automated cortical thickness estimation with histologic measures performed on two post-mortem brains, but a comparison between histologic measurements and FreeSurfer estimates obtained from in vivo MR was never performed.

Most of the surgical operations performed at the "Claudio Munari" Center for Epilepsy and Parkinson Surgery are brain resections aimed at treating drug resistant epilepsy. Since 2008 we have included FreeSurfer processing in our surgical

planning workflow (Cardinale et al. 2012, 2013). In fact, the reconstruction of the pial surface is helpful when planning both stereotactic implantation of intracerebral electrodes and brain resections. Moreover, cortical thickness maps are useful for localizing the central sulcus.

Given that all brain specimens are routinely sent for neuro-pathological examination, we had the unique opportunity of measuring the cortical thickness in vivo using FreeSurfer and ex vivo on the histologic specimen, after surgical resection. Thus, the goal of this method-comparison study was to validate the FreeSurfer estimated cortical thickness against histologic manual measurements in a series of brain tissue samples resected for the treatment of drug-resistant epilepsy. We also correlated cortical thickness with the patients' age and compared the mean thickness of the pathological and non-pathological specimens. Such ancillary analyses were performed in order to test the consistency of our data with previously published evidences (Salat et al. 2004; Colliot et al. 2006).

Materials and Methods

Subjects

Patients undergoing surgical treatment for drug-resistant epilepsy were considered for inclusion. Surgery was aimed at resecting the epileptogenic zone (EZ). EZ, as pre-surgically defined, included a MR-visible lesion in 20 of the 26 subjects. The planned resection included a large region free from any MR-visible abnormalities in all subjects. The inclusion criterion was the presence within the planned resection of areas of cortex, visually recognizable both by intraoperative direct visual inspection and by the 3D surface reconstruction, free from any MR-visible abnormalities. Exclusion criteria were the time lapse between the specimen excision and the tissue fixation exceeding 15 min, the presence of high-grade tumors and major technical artifacts affecting the histologic specimens.

Between January 2011 and January 2012, 113 consecutive subjects were operated on and considered for eligibility. Eighty-seven subjects were excluded according to the above-mentioned criteria. The study was thus performed on 27 histologic specimens from 26 patients (16 males; mean age (±Standard Deviation—SD) 28±13 years, range 4–52). Ten patients were affected by low-grade tumors (5 gangliogliomas, 2 DNT, 1 glioneuronal hamartoma, 1 xanthoastrocytoma pleomorphic, 1 pilocytic astrocytoma).

Data Acquisition

MR datasets were acquired with Achieva® 1.5 T magnet (Philips Healthcare; Best, The Netherlands) using eight channel coil and SENSE® technology. All patients underwent 3D-volume fast field echo (FFE) T1-weighted (T1W) imaging.

This dataset (contiguous axial slices with 560×560 matrix, $0.46 \times 0.46 \times 0.9$ mm voxel, without inter-slice gap) was stored for each patient on a Picture Archiving and Communication System. In our center, a 3D T1W sequence is routinely acquired for diagnostic evaluation in our center (Colombo et al. 2012), thus no extra-time acquisition was needed for the purpose of the present study. Only one 3D T1W sequence per patient was obtained. All the other acquired MR sequences were not relevant for the present study.

Data Processing

All patients were processed with automatic FreeSurfer "recon-all" pipeline. The surface-based stream implemented in FreeSurfer includes some preliminary steps, such as affine registration to Talairach atlas, bias correction and skull stripping. Subsequently, cutting planes are used to separate the hemispheres and to remove the brain stem and the cerebellum. Then the white matter and the pial surfaces are estimated. The accuracy of white-gray matter boundary and pial reconstructions was visually checked by the surgeons, particularly in the examined region (Fig. 1). Because FreeSurfer routinely has a hard limit of 5 mm on the cortical thickness, we ran the command "mris_thickness" with an optional parameter that allowed a maximum value of 10 mm. 3D brain surface reconstructions were obtained with different versions of FreeSurfer at the time of surgery. For cortical thickness estimation and final analysis all data were reprocessed with the same version of Freesurfer (5.1.0), according to the suggestions given by Gronenschild et al. (2012). The analysis was performed on Apple Mac Pro® workstations 2×2.26 GHz Quad-Core Intel Xeon (Cupertino, Silicon Valley, CA, USA), running OS X® 10.6.8. The mean time needed to compute the whole FreeSurfer pipeline was 12 h:57 m±2 h:6 m (SD).

Specimen Identification

Every Region Of Interest (ROI) was preliminarily identified in the surgical field (the exposed area of brain surface after the dura mater is opened), and then finally identified on both the corresponding resected specimen and on the FreeSurfer pial surface reconstruction (Fig. 2) with a multistep process:

1. Once the specimen was resected, it was visually compared with the FreeSurfer pial surface as shown by "tksurfer", the surface viewer provided by the software package.
2. The ROI was visually identified on both the FreeSurfer pial surface and on the surgical specimen surface.
3. The identified ROI was contoured as a manually user-defined label on the FreeSurfer pial surface with the drawing tools available in "tksurfer".
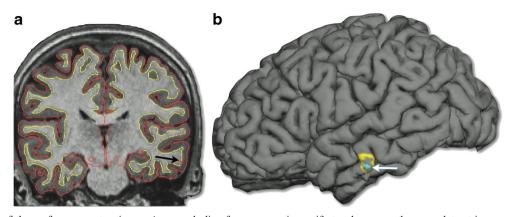4. The same ROI was contoured with black ink on the surgical specimen.

Fig. 1 Quality of the surface reconstruction. **a** A coronal slice from subject 1 (see Table 1) at the level of the Region Of Interest (ROI) 1 located on the middle temporal gyrus (see Table 2). The white (white/gray matter interface) and the pial surface are outlined in *yellow* and *red*, respectively. The high quality of the segmentation is clearly evident, despite the use of only one MR dataset (FreeSurfer can compensate motion artifacts when more than one dataset is processed). **b** The pial surface of the left hemisphere, with the yellow outline of the ROI 1. The same vertex (same ID) is indicated in **a** (*black arrow* on the white/gray matter interface indicating a red vertex) and in **b** (*white arrow* on the pial surface indicating a blue vertex). The quality of the surface reconstruction was visually checked for all subjects

The above-described process was completed as quickly as possible.

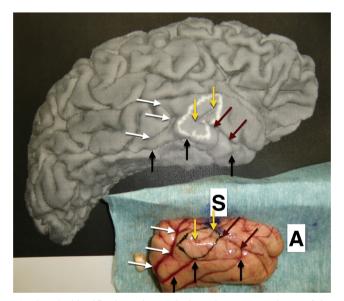It was possible to define multiple ROI on the same anatomical sample, for example on the gyral crown and on the sulcal bottom. ROI were defined only on apparently normal brain portions, according to MR and intra-operative macroscopical inspection, to avoid interferences with histologic diagnosis on presumably altered samples.

Histologic Examination and Measurements

Specimens were fixed in buffered 4 % formaline solution and paraffine-embedded. Four-micron thick sections were coronally cut from the ROI (marked with black ink), mounted on Superfrost Plus slides and counterstained with hematoxylin-eosin and Kluver-Barrera. The cortical thickness was measured using an Olympus BX40 microscope from the pial surface to the white/gray matter boundary with a 2× objective. The measurements were obtained ten times for every ROI, on several artifact-free optical fields, and the mean values were compared with the FreeSurfer estimates. The cortical thickness was measured drawing the rulers as perpendicular as possible to the pial surface as seen in each slice, along the direction of radial cortical vessels (Fig. 3).

Statistical Analysis

An agreement analysis between FreeSurfer estimation and histologic examination for measuring the cortical thickness was performed using Passing–Bablok regression analysis (Passing and Bablok 1983, 1984) and Bland–Altman plot (Bland and Altman 1986).

Moreover, some related and ancillary analyses were performed. The Shapiro–Wilk method was used to test the normality of thickness values. Mean values of cortical thickness were compared with two-tailed, paired-samples t-test. The correlation between thickness and age was evaluated with the Pearson's product-moment correlation test.

Fig. 2 ROI identification. The surgical specimen (external part of the right temporal lobe, including the middle temporal, the inferior temporal and the fusiform gyri) is oriented on a piece of paper (*A* = anterior; *S* = superior) and compared with the FreeSurfer reconstruction of the pial surface of the right hemisphere. The corresponding ROI (including a portion of the middle and of the inferior temporal gyri) are drawn with black ink on the surgical specimen and contoured with a white line on the reconstructed pial surface. The surgical specimens were usually positioned close to the computer monitor for the visual comparison. This FreeSurfer reconstruction was printed on paper for editing the figure. The visual comparison is suboptimal because the specimen flattens when lying on the table and because of small distortions introduced by the software. The *arrows* indicate corresponding positions: *black arrows* on the lateral temporo-occipital sulcus; *brown arrows* on the inferior temporal sulcus; *yellow arrows* on a small sulcus inside the ROI; *white arrows* on a sulcus posterior to the ROI
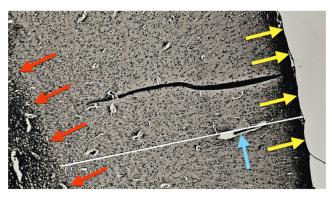
Fig. 3 Manual measurement on the histologic specimen. The ruler (*white line*) is drawn between the pial surface (*yellow arrows*) and the gray/white matter surface (*red arrows*). Radial cortical vessels (*blue arrow*) were helpful for positioning the ruler perpendicularly to the pial surface

The statistical analysis was performed with R 2.15.1 (R Development Core Team 2012).

Approvals and Informed Consent

The use of FreeSurfer as a complementary tool for clinical purposes (given that all conventional certified tools are used) was approved by the Niguarda Hospital Institutional Review Board. The local Ethical Committee approved this study. The analysis of the brain specimens for research purposes was performed after a specific informed consent was obtained from all patients or their guardians.
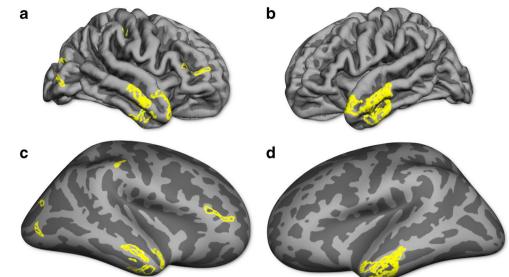
Results

Twenty-seven ROI from 26 subjects were analyzed. Demographic and main clinical–pathological data are reported in Table 1. The position of the 27 ROI is depicted in Fig. 4. Seven of the 27 specimens examined presented pathological

Table 1 Demographic and clinical–pathological data

Subject ID	Sex	Age	MRI	Side	Surgery	Histologic diagnosis
1	F	48	Positive	L	Antero-mesial temporal lobectomy	Ganglioglioma
2	F	38	Positive	L	Antero-mesial temporal lobectomy	DNT
3	M	26	HS	L	Antero-mesial temporal lobectomy	FCD IIIa
4	M	29	Positive	R	Antero-mesial temporal lobectomy	Ganglioglioma
5	F	17	Negative	R	Temporo-occipital cortectomy	FCD IIb
6	F	9	HS	L	Antero-mesial temporal lobectomy	HS
7	M	32	HS	R	Antero-mesial temporal lobectomy	HS
8	F	39	HS	L	Antero-mesial temporal lobectomy	HS
9	M	47	Positive	R	Temporo-occipital lobectomy	Periventricular nodular heterotopia
10	M	30	HS	R	Antero-mesial temporal lobectomy	HS
11	M	43	HS	R	Antero-mesial temporal lobectomy	FCD IIIa
12	M	19	Positive	R	Frontal lobectomy	FCD IIa
13	F	13	Positive	L	Temporo-occipital lobectomy	FCD IIb
14	F	4	Negative	R	Central cortectomy	Glioneuronal hamartoma
15	M	22	Negative	R	Temporo-opercular cortectomy	FCD I
16	M	28	Negative	L	Antero-mesial temporal lobectomy	Negative
17	F	46	Positive	L	Antero-mesial temporal lobectomy	FCD IIIb (Xanthoastrocytoma pleomorphic)
18	M	19	Positive	L	Antero-mesial temporal lobectomy	Ganglioglioma
19	F	19	Negative	R	Temporo-insular lobectomy	Negative
20	M	14	Positive	L	Antero-mesial temporal lobectomy	FCD IIIb (Ganglioglioma)
21	M	39	HS	R	Antero-mesial temporal lobectomy	HS
22	M	10	Negative	L	Antero-mesial temporal lobectomy	Negative
23	M	52	Positive	R	Antero-mesial temporal lobectomy	FCD IIIb (DNT)
24	M	18	Positive	R	Antero-mesial temporal lobectomy	Pilocytic astrocytoma
25	F	37	HS	R	Antero-mesial temporal lobectomy	FCD IIIa
26	M	27	Positive	L	Antero-mesial temporal lobectomy	Ganglioglioma

Histologic diagnosis is the result of the analysis of all resected specimens. In some cases the patient-specific histologic diagnosis is therefore not the same as in Table 2, where the specimen-specific diagnosis is reported. Mean age (±SD) is 27.9 (±13.4) years. Focal Cortical Dysplasias (FCD) are classified according to Blümcke et al. (2011)

MRI findings: Negative = no abnormalities; Positive = evidence of structural abnormalities other than HS; HS = evidence of Hippocampal Sclerosis

DNT Dysembryoplastic Neuroepithelial Tumour

Fig. 4 The position of the 27 ROI reported on the brain surface of the "fsaverage" subject, a common space provided by FreeSurfer. All subjects were non-linearly registered to fsaverage, and all labels were loaded on its surface. The labels are located on the pial surface (**a**, right side, and **b**, left side) and on the inflated surface (**c**, right side, and **d**, left side). *Light gray* defines the crowns of the gyri, *dark gray* the sulci. Most labels are positioned in the temporal lobe and overlap each other

abnormalities not recognizable on the corresponding MR images. Six were focal cortical dysplasias (FCD), one was a glioneuronal hamartoma.

Measurements and related data from the 27 specimens are reported in Table 2.

The mean cortical thickness values (±SD) obtained with FreeSurfer and with the histologic measurements were 3.65 mm±0.44 and 3.72 mm±0.36, respectively (P value (P)=0.32). Both series of values were normally distributed (P=0.67 and P=0.28, respectively). In 17 of 27 records the histologic measurement was greater than the FreeSurfer estimation. The cortical thickness never exceeded the value of 5 mm with both methods.

A scatter plot comparing the two measurements, along with the Passing–Bablok regression line, is depicted in Fig. 5: the intercept and the slope values (with the 95 % Confidence Interval (CI)) are −1.37 (−5.36, 0.53) and 1.34 (0.83, 2.44), respectively.

The Bland–Altman plot is depicted in Fig. 6: the mean of the measurement differences is −0.07 mm, and the 95 % CI ranges from −0.79 to 0.65 mm (range=1.44 mm). The distribution of circles shows the random nature of the errors, suggesting the absence of any bias.

Some subgroup analyses were also performed. In the subgroup of the 20 specimens without any histologic abnormalities, the mean cortical thickness values (±SD) obtained with FreeSurfer and histologic measurement were 3.63 mm±0.46 and 3.72 mm±0.36, respectively (P=0.21). In the subgroup of the seven specimens with some histologic abnormalities, the mean cortical thickness values (±SD) obtained with FreeSurfer and histologic measurement were 3.72 mm±0.43 and 3.71 mm ±0.41, respectively (P=0.96). FreeSurfer thickness estimations were inversely correlated to the age of the patients (correlation index c=−0.36), with a trend towards statistical significance (P=0.06). Moreover, the mean thickness values (±SD) of non-

pathological specimens and pathological specimens (6 FCD and 1 glioneuronal hamartoma) were 3.63±0.46 mm and 3.72±0.43 mm, respectively (P=0.62). Similar results were obtained with histologic measurements: the thickness values were inversely correlated to age (c=−0.25), but without any trend towards statistical significance (P=0.2). The mean thickness values (±SD) of non-pathological specimens and of pathological specimens were 3.72±0.36 mm and 3.71±0.41 mm, respectively (P=0.96).

Discussion

Cortical thickness measurements have been used to study a wide variety of psychiatric and neurologic disorders ranging from schizophrenia to neuropathic trigeminal pain. The studies on cortical thickness changes associated to epilepsy are numerous and closer to the main field of interest of our center. Such morphometric studies were performed on the cortical malformations of affected subjects (Antel et al. 2003; Colliot et al. 2006; Oliveira et al. 2010; Thesen et al. 2011), but also in cases of temporal (McDonald et al. 2008; Labate et al. 2011) and frontal epilepsies (Widjaja et al. 2011).

FreeSurfer has been used in a number of studies for estimating the brain cortical thickness. These estimations were proved to fall within expected range (Fischl and Dale 2000) and were compared with manual measurements performed both in 32 healthy and 33 schizophrenic subjects (Kuperberg et al. 2003), or in the context of a longitudinal study on age-related thinning (Salat et al. 2004). Moreover, Rosas et al. (2002) computed thickness values against histologic measures in the same tissue samples: they used ten MR scans for both one post-mortem healthy brain and one post-mortem Huntington Disease (HD) affected brain. The cortical thickness was measured with both FreeSurfer and the traditional histologic

Table 2 Measurements and related data

ROI ID	Subject ID	Specimen topography	Specimen pathology	Site of measurement	Vertices	Area (mm²)	FreeSurfer (mm ± SD)	Histology (mm ± SD)	Histology—FreeSurfer (mm)
1	1	Anterior T2	None	Crown	332	400	3.44±0.51	3.82±0.41	0.39
2	2	Middle T2	None	Crown	172	248	3.38±0.37	3.77±0.11	0.39
3	3	Anterior T2–T3	FCD I	Crown	906	798	3.45±0.61	3.61±0.27	0.16
4	4	Anterior T2	None	Crown	89	168	3.87±0.52	3.94±0.14	0.08
5	5	O2	FCD IIb	Crown	165	143	3.06±0.42	3.18±0.23	0.12
6	6	Temporal pole	None	Crown	82	225	4.47±0.47	4.48±0.25	0.01
6 bis	6	Anterior T2	None	Crown	70	167	4.60±0.39	4.38±0.25	−0.22
7	7	Anterior T2	None	Crown	132	200	3.69±0.28	4.03±0.27	0.35
8	8	Temporal pole	None	Crown	360	355	3.26±0.42	3.49±0.20	0.23
9	9	Gyrus angularis	None	Sulcus	215	156	2.99±0.43	2.83±0.26	−0.16
10	10	Middle T2	None	Crown-Sulcus Transition	266	331	3.45±0.45	3.98±0.38	0.53
11	11	Temporal pole	None	Crown	221	182	3.38±0.39	3.58±0.27	0.21
12	12	Anterior/middle F2	None	Crown-Sulcus Transition	557	719	2.81±0.61	3.60±0.40	0.80
13	13	Middle T2	FCD IIb	Crown	158	260	4.27±0.46	4.38±0.15	0.11
14	14	Middle parietal ascending gyrus—anterior P2	Glioneuronal hamartoma	Crown-Sulcus Transition	91	118	3.76±0.54	3.60±0.33	−0.16
15	15	Anterior T3	None	Crown	88	125	3.49±0.23	3.58±0.21	0.10
16	16	Temporal pole	None	Crown	212	257	3.18±0.42	3.32±0.37	0.14
17	17	Anterior T2–T3	None	Crown	146	188	3.81±0.40	3.69±0.20	−0.12
18	18	Anterior T2–T3	None	Crown	98	125	3.85±0.24	3.48±0.13	−0.38
19	19	Anterior T3	None	Crown	120	215	3.77±0.63	3.59±0.39	−0.18
20	20	Middle T2	FCD I	Crown	72	124	3.87±0.33	3.68±0.15	−0.19
21	21	Anterior T3	None	Crown	73	149	4.26±0.37	3.64±0.28	−0.62
22	22	Anterior T3	None	Crown	65	101	3.84±0.40	3.61±0.23	−0.23
23	23	Anterior T1	FCD I	Crown	212	332	3.48±0.47	4.13±0.25	0.66
24	24	Anterior T3	None	Crown	58	84	3.58±0.26	3.88±0.39	0.30
25	25	Anterior T3–T4	FCD IIa	Crown	66	126	4.17±0.49	3.42±0.62	−0.75
26	26	Middle T3	None	Crown	74	86	3.42±0.37	3.75±0.36	0.33

The median number of vertices per specimen (and relative measurements) is 132 (InterQuartile range 78–213.5)

FCD are classified according to Blümcke et al. (2011). T1 = Superior Temporal Gyrus. T2 = Middle Temporal Gyrus. T3 = Inferior Temporal Gyrus. T4 = Fusiform Gyrus. O2 = Middle Occipital Gyrus. P2 = Inferior Parietal Lobule. The reported histological diagnosis is specifically related to the specimens used for measurements. Histologic measurements were obtained ten times for each ROI, and the mean ± SD is reported. ROI 6 and 6bis were obtained both from subject 6

technique at different locations, and the results agreed to within 0.2 mm (mean difference 0.077 mm). This study, performed in the context of a longitudinal study regarding cortical thinning in HD, confirmed the high accuracy of the automated thickness estimation, but it relied on post-mortem and ten repeated MR scans of two specimens from two brains.

The findings of the present study indicate a good agreement between FreeSurfer estimates and histologic measurements of the cortical thickness. These results derive from the statistical analysis performed with two methods specifically developed for method-comparison studies. Passing–Bablok linear regression is a non-parametric analysis, more appropriate than Pearson's product-moment correlation test for method comparison studies (Passing and Bablok 1983, 1984). The intercept of the regression line assesses the systematic bias: a CI below zero denotes a constant underestimation trend whereas values over zero denote an overestimation trend. In the present study the CI includes zero, suggesting that there is not any significant systematic bias. The slope of the regression line assesses the proportional bias: in the present study its CI includes 1, indicating a good agreement between the two methods. We compared the two methods also computing the Bland–Altman plot. The mean of the differences is −0.07, indicating once more a good agreement between the two methods. This graphical technique shows that the 95 % CI ranges from −0.79 to 0.65 mm, including the perfect identity line (where the difference is 0). The two methods are obviously not clinical alternatives, because histologic measurement cannot be part of the
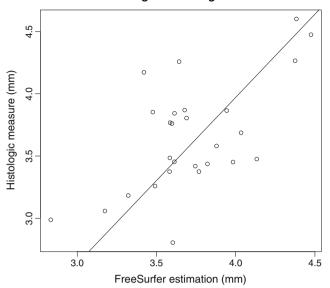
Passing-Bablok Regression

Fig. 5 Scatter plot with Passing–Bablok regression line. The graph shows the good agreement between FreeSurfer estimates and histologic measurements of cortical thickness

presurgical diagnostic evaluation. Nevertheless, our findings contribute to validate the FreeSurfer estimates, especially if we consider certain specific pathological conditions, such as FCD. In fact, the 95 % CI range is 1.44 mm, a value that does not appear relevant when estimating regional thickness changes related to the presence of FCD. Colliot et al. reported in 2006 the comparison of cortical thickness values (MR manual measurements) between 23 FCD affected subjects and 39 healthy controls. They found that 56 % of FCD subjects had thickness values greater than 6 mm, while normal subjects never
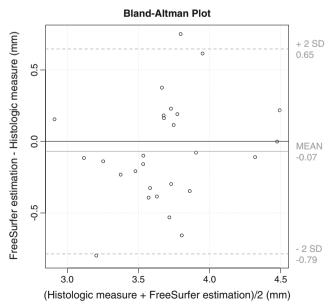
Bland-Altman Plot

Fig. 6 Bland–Altman plot. The perfect identity line (*black line*) and all but two plots are included in the 95 % Confidence Interval (*dotted lines*), suggesting a good agreement between the two methods

exceeded the value of 4.5 mm. In the present study the difference between the two methods lies within the 1.44 mm range, probably small enough to avoid obscuring eventual true differences between clinical groups. We therefore are encouraged to use FreeSurfer in the future to investigate the morphometric properties of FCD and its usefulness for detecting dysplastic lesions that are difficult to see on conventional MR visual inspection.

Mean cortical thickness values obtained in our study were generally higher with histologic measurements. This finding agrees with our expectations because the manual measurements on histologic slices tend to give higher values due to the difficulty of drawing the rulers perfectly orthogonal to the pial surface. This source of error is likely partially compensated by the tissue shrinkage after formaline fixation.

Seven of the 27 specimens analyzed in this study presented unexpected, MR-occult pathologies in the area chosen for morphometric evaluation. The mean cortical thickness of these seven specimens did not differ from non-pathological specimens, but it must be argued that the very small sample size lowers the power of the analysis. Moreover, this analysis compared normal specimens with subtle FCD-affected specimens, and there is still lack of information regarding morphometric properties of these MR-undetectable lesions.

The difference between FreeSurfer and histologic measurements is slightly greater than reported by Rosas et al. in 2002. This is mainly due to the different experimental setup: our measures were obtained in standard clinical conditions, while they performed ten MR scans on post-mortem fixed brains.

The major strength of our study is that, to the best of our knowledge, it is the only one that validates FreeSurfer cortical thickness estimates computed from a single MR scan per subject, obtained in vivo and in conventional diagnostic conditions, against ex vivo histologic measurements obtained from the same cases at same locations.

The major limitation of this study is the biased topography of examined brain tissue, with most samples resected from the lateral aspect of the temporal lobe. Another potential limitation is that only one MR data set was obtained and processed for every subject, due to time constraints during the acquisition aimed at diagnostic evaluation. In fact, it is a general recommendation that more than one acquisition is used with FreeSurfer, increasing the signal-to-noise ratio and reducing the effect of motion artifacts. Nevertheless, the processing resulted in high quality surface reconstructions (Fig. 1). Moreover, the FreeSurfer thickness was not verified at histology on a vertex-by-vertex basis, but it must be considered that, given how small the ROI are, this does not invalidate the conclusions.

To further explore the clinical usefulness in epilepsy surgery, we are planning to measure cortical thickness with FreeSurfer in a large series of histologically proven FCD.

Conclusions

There is a good agreement between FreeSurfer estimations and histologic measurements of cortical thickness. FreeSurfer can be considered a reliable tool for this kind of computation, and it could be helpful in the presurgical workup of many pathological conditions such as FCD in epileptic patients.

Information Sharing Statement

FreeSurfer (RRID:nif-0000-00304) software is publicly and freely available from the FreeSurferWiki resource (http://surfer.nmr.mgh.harvard.edu/fswiki/FreeSurferWiki), which is developed and maintained at the Martinos Center for Biomedical Imaging (http://www.nmr.mgh.harvard.edu/martinos/noFlashHome.php). All software, information and support are provided online at the FreeSurferWiki webpage.

Disclosures   The Authors have nothing to disclose.

References

Antel, S. B., Collins, D. L., Bernasconi, N., Andermann, F., Shinghal, R., Kearney, R. E., et al. (2003). Automated detection of focal cortical dysplasia lesions using computational models of their MRI characteristics and texture analysis. *NeuroImage, 19*(4), 1748–1759.

Bland, J. M., & Altman, D. G. (1986). Statistical methods for assessing agreement between two methods of clinical measurement. *The Lancet, 327*(8476), 307–310.

Blümcke, I., Thom, M., Aronica, E., Armstrong, D. D., Vinters, H. V., Palmini, A., et al. (2011). The clinicopathologic spectrum of focal cortical dysplasias: a consensus classification proposed by an ad hoc Task Force of the ILAE Diagnostic Methods Commission. *Epilepsia, 52*(1), 158–174.

Cardinale, F., Miserocchi, A., Moscato, A., Cossu, M., Castana, L., Schiariti, M. P., et al. (2012). Talairach methodology in the multimodal imaging and robotics era. In J.-M. Scarabin (Ed.), *Stereotaxy and epilepsy surgery* (pp. 245–272). Montrouge: John Libbey Eurotext.

Cardinale, F., Cossu, M., Castana, L., Casaceli, G., Schiariti, M. P., Miserocchi, A., et al. (2013). Stereoelectroencephalography: surgical methodology, safety, and stereotactic application accuracy in 500 procedures. *Neurosurgery, 72*(3), 353–366.

Colliot, O., Antel, S. B., Naessens, V. B., Bernasconi, N., & Bernasconi, A. (2006). In vivo profiling of focal cortical dysplasia on high-resolution MRI with computational models. *Epileptic Disorders: International Epilepsy Journal with Videotape, 47*(1), 134–142.

Colombo, N., Tassi, L., Deleo, F., Citterio, A., Bramerio, M., Mai, R., et al. (2012). Focal cortical dysplasia type IIa and IIb: MRI aspects in 118 cases proven by histopathology. *Neuroradiology, 54*(10), 1065–1077.

Dale, A. M., Fischl, B., & Sereno, M. I. (1999). Cortical surface-based analysis. I. Segmentation and surface reconstruction. *NeuroImage, 194*, 179–194.

Fischl, B. (2012). FreeSurfer. *NeuroImage, 62*, 774–781.

Fischl, B., & Dale, A. M. (2000). Measuring the thickness of the human cerebral cortex from magnetic resonance images. *Proceedings of the National Academy of Sciences of the United States of America, 97*(20), 11050–11055.

Fischl, B., Liu, A. K., & Dale, A. M. (2001). Automated manifold surgery: constructing geometrically accurate and topologically correct models of the human cerebral cortex. *IEEE Transactions on Medical Imaging, 20*(1), 70–80.

Gronenschild, E. H. B. M., Habets, P., Jacobs, H. I. L., Mengelers, R., Rozendaal, N., van Os, J., et al. (2012). The effects of FreeSurfer Version, Workstation Type, and Macintosh Operating System Version on anatomical volume and cortical thickness measurements. *PLoS ONE, 7*(6), e38234.

Kuperberg, G. R., Broome, M. R., McGuire, P. K., David, A. S., Eddy, M., Ozawa, F., et al. (2003). Regionally localized thinning of the cerebral cortex in schizophrenia. *Archives of General Psychiatry, 60*(9), 878–888.

Labate, A., Cerasa, A., Aguglia, U., Mumoli, L., Quattrone, A., & Gambardella, A. (2011). Neocortical thinning in "benign" mesial temporal lobe epilepsy. *Epilepsia, 52*(4), 712–717.

McDonald, C. R., Hagler, D. J., Ahmadi, M. E., Tecoma, E., Iragui, V., Gharapetian, L., et al. (2008). Regional neocortical thinning in mesial temporal lobe epilepsy. *Epilepsia, 49*(5), 794–803.

Oliveira, P. P. D. M., Valente, K. D., Shergill, S. S., Leite, C. D. C., & Amaro, E. (2010). Cortical thickness reduction of normal appearing cortex in patients with polymicrogyria. *Journal of Neuroimaging: Official journal of the American Society of Neuroimaging, 20*(1), 46–52.

Passing, H., & Bablok, W. (1983). A new biometrical procedure for testing the equality of measurements from two different analytical methods. Application of linear regression procedures for method comparison studies in clinical chemistry, part I. *Journal of Clinical Chemistry and Clinical Biochemistry. Zeitschrift für Klinische Chemie und Klinische Biochemie, 21*, 709–720.

Passing, H., & Bablok, W. (1984). A new biometrical procedure for testing the equality of measurements from two different analytical methods. Application of linear regression procedures for method comparison studies in clinical chemistry, part II. *Journal of Clinical Chemistry and Clinical Biochemistry. Zeitschrift für Klinische Chemie und Klinische Biochemie, 22*, 431–445.

R Development Core Team (2012). R: A language and environment for statistical computing. R Foundation for Statistical Computing, Vienna, Austria. ISBN 3-900051-07-0, URL http://www.R-project.org/. Accessed 01 Nov 2012.

Rosas, H. D., Liu, A. K., Hersch, S. M., Glessner, M., Ferrante, R. J., Salat, D. H., et al. (2002). Regional and progressive thinning of the cortical ribbon in Huntington's disease. *Neurology, 58*, 695–701.

Salat, D. H., Buckner, R. L., Snyder, A. Z., Greve, D. N., Desikan, R. S. R., Busa, E., et al. (2004). Thinning of the cerebral cortex in aging. *Cerebral Cortex, 14*(7), 721–730.

Thesen, T., Quinn, B. T., Carlson, C., Devinsky, O., DuBois, J., McDonald, C. R., et al. (2011). Detection of epileptogenic cortical malformations with surface-based MRI morphometry. *PLoS ONE, 6*(2), 1–10.

Widjaja, E., Mahmoodabadi, S. Z., Snead, O. C., Almehdar, A., & Smith, M. L. (2011). Widespread cortical thinning in children with frontal lobe epilepsy. *Epilepsia, 52*(9), 1685–1691.